Kobe University Repository : Kernel

PDF issue: 2025-12-04

Electronic coupling calculations with transition charges, dipoles, and quadrupoles derived from electrostatic potential fitting

Fujimoto, Kazuhiro.J

(Citation)
Journal of Chemical Physics,141:214105-214105

(Issue Date)
2014

(Resource Type)
journal article

(Version)
Version of Record

(URL)
https://hdl.handle.net/20.500.14094/90002665

AIP | The Journal of Chemical Physics

Electronic coupling calculations with transition charges, dipoles, and quadrupoles derived from electrostatic potential fitting

Kazuhiro J. Fujimoto

Citation: The Journal of Chemical Physics **141**, 214105 (2014); doi: 10.1063/1.4902758
View online: http://dx.doi.org/10.1063/1.4902758
View Table of Contents: http://scitation.aip.org/content/aip/journal/jcp/141/21?ver=pdfcov
Published by the AIP Publishing

Articles you may be interested in

Molecular near-field antenna effect in resonance hyper-Raman scattering: Intermolecular vibronic intensity borrowing of solvent from solute through dipole-dipole and dipole-quadrupole interactions
J. Chem. Phys. **140**, 204506 (2014); 10.1063/1.4879058

A new ab initio intermolecular potential energy surface and predicted rotational spectra of the Kr−H2O complex
J. Chem. Phys. **137**, 224314 (2012); 10.1063/1.4770263

Development of the isotropic site-site potential for exchange repulsion energy and combination with the isotropic site-site potential for electrostatic part
J. Chem. Phys. **137**, 204101 (2012); 10.1063/1.4766312

Electronic coupling matrix elements from charge constrained density functional theory calculations using a plane wave basis set
J. Chem. Phys. **133**, 244105 (2010); 10.1063/1.3507878

Nuclear quadrupole coupling in Cl 2 C=CHCl and Cl 2 C=CH 2 : Evidence for systematic differences in orientations between internuclear and field gradient axes for terminal quadrupolar nuclei
J. Chem. Phys. **109**, 10263 (1998); 10.1063/1.477722

This article is copyrighted as indicated in the article. Reuse of AIP content is subject to the terms at: http://scitation.aip.org/termsconditions. Downloaded to IP: 133.30.52.204 On: Thu, 04 Dec 2014 05:09:54

THE JOURNAL OF CHEMICAL PHYSICS **141**, 214105 (2014)

Electronic coupling calculations with transition charges, dipoles, and quadrupoles derived from electrostatic potential fitting

Kazuhiro J. Fujimoto[a)]
Department of Computational Science, Graduate School of System Informatics, Kobe University, 1-1, Rokkodai, Nada, Kobe 657-8501, Japan

(Received 29 August 2014; accepted 14 November 2014; published online 2 December 2014)

A transition charge, dipole, and quadrupole from electrostatic potential (TrESP-CDQ) method for electronic coupling calculations is proposed. The TrESP method is based on the classical description of electronic Coulomb interaction between transition densities for individual molecules. In the original TrESP method, only the transition charge interactions were considered as the electronic coupling. In the present study, the TrESP method is extended to include the contributions from the transition dipoles and quadrupoles as well as the transition charges. Hence, the self-consistent transition density is employed in the ESP fitting procedure. To check the accuracy of the present approach, several test calculations are performed to a helium dimer, a methane dimer, and an ethylene dimer. As a result, the TrESP-CDQ method gives a much improved description of the electronic coupling, compared with the original TrESP method. The calculated results also show that the self-consistent treatment to the transition densities contributes significantly to the accuracy of the electronic coupling calculations. Based on the successful description of the electronic coupling, the contributions to the electronic coupling are also analyzed. This analysis clearly shows a negligible contribution of the transition charge interaction to the electronic coupling. Hence, the distribution of the transition density is found to strongly influence the magnitudes of the transition charges, dipoles, and quadrupoles. The present approach is useful for analyzing and understanding the mechanism of excitation-energy transfer. © *2014 AIP Publishing LLC*. [http://dx.doi.org/10.1063/1.4902758]

I. INTRODUCTION

Electronic coupling is an intermolecular interaction between different electronic states.[1,2] The magnitude of the electronic coupling is known to strongly influence a rate constant of excitation-energy transfer (EET), so that the accurate description of the electronic coupling has a significant role in EET studies. The rate constant of EET was first derived by Förster.[3] In this theory, the electronic coupling required for the EET rate was reduced to the Coulomb coupling and hence it was approximated to a dipole-dipole (dd) interaction using transition dipole moments for individual molecules. The dd method is easily applicable to the electronic coupling calculations because of its simplicity. Hence this method provides an intuitive interpretation of the electronic coupling. Owing to these features, the dd method has been widely used for EET studies.[1] However, the utility of the dd method is limited to the case where the intermolecular separation between two interacting molecules is larger than their molecular sizes.[1,2] Therefore, the dd method must be used with care.

To circumvent this problem, many theoretical studies have been performed.[4–25] As a pioneering study, Krueger *et al.* proposed a transition density cube (TDC) method,[9] in which the electronic coupling was quantum-mechanically calculated with transition densities. A transition-density-fragment interaction (TDFI) method[26–29] was proposed as a similar approach to the TDC method. The difference between the two methods is in the treatment of transition densities. In the TDFI method, the electronic coupling is calculated with self-consistent transition densities that are obtained from a density-fragment interaction (DFI) method.[30] The DFI method employs a mean-field treatment of interfragment interactions, so that the electron density interactions between individual molecules are iteratively calculated until the total energy is converged. On the other hand, the TDC method employs the transition densities obtained from isolated monomer calculations, in which intermolecular interaction is not considered. In the previous studies, the TDFI method was applied to EET,[26,28] exciton-coupled circular dichroism spectra,[27] and crystallochromy.[29] As a result, TDFI successfully reproduced the experimental values of the electronic couplings. These studies also showed a significant role of the self-consistent procedure by the DFI method in the quantitative description of the electronic coupling.

Madjet *et al.* proposed an alternative approach for the electronic coupling calculations, called a transition charge from electrostatic potential (TrESP) method.[16] The basic idea of this method comes from a transition monopole approximation.[4] In the TrESP method, the electronic coupling is evaluated as classical Coulomb interactions between transition charges and the values of the transition charges are derived from electrostatic potential (ESP) fitting.[31,32] While the transition dipoles in the dd method are located on the molecular centers, the TrESP method employs the transition charges distributed on the individual atoms in the interacting molecules. Such multicenter interactions in TrESP led to a

[a)]Electronic mail: fujimoto@ruby.kobe-u.ac.jp.

 © 2014 AIP Publishing LLC

This article is copyrighted as indicated in the article. Reuse of AIP content is subject to the terms at: http://scitation.aip.org/termsconditions. Downloaded to IP: 133.30.52.204 On: Thu, 04 Dec 2014 05:09:54

much improved description of the electronic coupling, compared with the dd method. However, the TrESP method is still insufficient to achieve the TDFI accuracy. Two reasons are considered; one is the description based only on the monopole charge interactions, alternatively, the lack of consideration of the self-consistent transition density could be also problematic.

This study attempts to extend the TrESP method in two ways. First, the present TrESP method includes not only the transition monopole charge interactions but also the higher order multipole (transition dipole and quadrupole) ones. Second, the self-consistent transition density is employed in the ESP fitting procedure. The present approach is called the transition charge, dipole, and quadrupole from ESP (TrESP-CDQ) method. For checking the accuracy of the present approach, several test calculations are performed. In this step, the TDFI calculations are also performed to obtain the reference values. As a result of the testing, the TrESP-CDQ method gives almost the same values as the TDFI method, while the original TrESP method completely fails in describing the reference values. Based on the successful description of the reference values, the effect of the self-consistent treatment and the contributions from the transition charges, dipoles, and quadrupoles are also explored.

II. THEORY

A. Electronic coupling

First, let us consider the total Hamiltonian for A-B molecular complex,

$$\hat{H} = \hat{H}_A + \hat{H}_B + \hat{V}_{AB}, \tag{1}$$

and the basis functions

$$\begin{aligned} |\Phi_1\rangle &= \left|\Psi_p^A \cdot \Psi_0^B\right\rangle, \\ |\Phi_2\rangle &= \left|\Psi_0^A \cdot \Psi_q^B\right\rangle. \end{aligned} \tag{2}$$

In Eq. (1), $\hat{H}_X$ denotes the local Hamiltonian for the molecule X ($X = A$ or B) and $\hat{V}_{AB}$ is the Coulomb interaction between the molecules A and B. In Eq. (2), Ψ_0^X and Ψ_p^X represent the ground state and the pth excited state for the molecule X, respectively. The electronic coupling between the molecules A and B is defined by an off-diagonal element of the Hamiltonian matrix. For a negligible overlap between the two basis functions, this matrix element is described as[33,34]

$$\begin{aligned} \langle\Phi_1|\hat{H}|\Phi_2\rangle &= \langle\Phi_1|\hat{V}_{AB}|\Phi_2\rangle \\ &= \int \mathrm{d}\mathbf{r}_1 \int \mathrm{d}\mathbf{r}'_1 \frac{\rho_{p0}^{A*}(\mathbf{r}_1)\rho_{q0}^{B}(\mathbf{r}'_1)}{|\mathbf{r}_1 - \mathbf{r}'_1|} \equiv V_{\mathrm{Coul}}. \end{aligned} \tag{3}$$

Here, a one-electron transition density of the molecule X, $\rho_{p0}^X(\mathbf{r})$, is introduced, which is defined by

$$\begin{aligned} \rho_{p0}^X(\mathbf{r}_1) \equiv N_{\mathrm{e}}^X \int \mathrm{d}s_1 \int \mathrm{d}\mathbf{x}_2 \ldots \\ \times \int \mathrm{d}\mathbf{x}_{N_{\mathrm{e}}^X} \Psi_p^X(\mathbf{x}_1, \mathbf{x}_2, \ldots, \mathbf{x}_{N_{\mathrm{e}}^X}) \Psi_0^{X*}(\mathbf{x}_1, \mathbf{x}_2, \ldots, \mathbf{x}_{N_{\mathrm{e}}^X}), \end{aligned} \tag{4}$$

where N_{e}^X denotes the number of electrons in the molecule X and $\mathbf{x}_i$ expresses space and spin coordinates of the ith electron, i.e., $\mathbf{x}_i \equiv (\mathbf{r}_i, s_i)$. For $p = 0$, Eq. (4) becomes the one-electron ground-state density. Equation (3) stands for the Coulomb interaction between the two transition densities. In this paper, this interaction is called the electronic coupling and it is represented by V_{Coul}. Although the exchange interaction is also included in the electronic coupling, this contribution is usually negligible.[28,35] Therefore, the present study focuses only on the Coulomb interaction. It is noted that the basis functions $|\Phi_1\rangle$ and $|\Phi_2\rangle$ in Eq. (2) correspond to local excitations (LE) within the molecule X. Therefore, the direct coupling between $|\Phi_1\rangle$ and $|\Phi_2\rangle$ is considered in Eq. (3). Although the indirect coupling via intermediate charge-transfer (CT) states is known to influence the amount of electronic coupling,[35,36] this contribution cannot be evaluated with Eq. (3) because the CT basis functions are not considered in Eq. (2). The indirect coupling is an interesting topic but this study does not focus on it. It is also noted that Eq. (3) corresponds to an intermolecular electrostatic energy in the case of $p = q = 0$. Therefore, the electronic coupling has a similar form to the intermolecular electrostatic energy.

B. Electronic coupling calculations with transition charges, dipoles, and quadrupoles

The intermolecular electrostatic energy between the molecules A and B, which are separated by $R_{ij} = |\mathbf{r}_i^A - \mathbf{r}_j^B|$, is classically described as[37,38]

$$\begin{aligned} E_{AB}^{\mathrm{ES}} = \sum_{l\in A} \sum_{l'\in B} \sum_{\alpha,\cdots,\nu'} \\ \times \frac{(-1)^l}{(2l-1)!!(2l'-1)!!} M_{\alpha\cdots\nu}^{(l)} T_{ij,\alpha\cdots\nu\alpha'\cdots\nu'} M_{\alpha'\cdots\nu'}^{(l')}, \end{aligned} \tag{5}$$

where $M_{\alpha\cdots\nu}^{(l)}$ (or $M_{\alpha'\cdots\nu'}^{(l')}$) denotes a multipole moment for the molecule A (or B) and l is the rank of the multipole. For example, $M_{\alpha\cdots\nu}^{(l)}$ for $l = 0$, 1, and 2 correspond to a monopole charge, a dipole moment, and a quadrupole moment, respectively. Greek letter in Eq. (5) denotes the tensor components, i.e., $\alpha = x, y$, or z. The symbol $(2l-1)!!$ expresses the product of odd integers, i.e., $(2l-1)!! \equiv 1 \times 3 \times 5 \cdots \times (2l-1)$. The tensor $T_{ij,\alpha\beta\gamma\cdots\nu}$ is a function of the intermolecular separation ($T_{ij} = R_{ij}^{-1}$), which is given by

$$T_{ij,\alpha\beta\gamma\cdots\nu} = \frac{\partial}{\partial R_{ij,\alpha}} \frac{\partial}{\partial R_{ij,\beta}} \frac{\partial}{\partial R_{ij,\gamma}} \cdots \frac{\partial}{\partial R_{ij,\nu}} T_{ij}. \tag{6}$$

In Eq. (5), the electrostatic energy is written as the sum of the Coulomb interactions between the multipoles for the molecules A and B. It is noted that these multipoles are located on the molecular centers $\mathbf{r}_i^A$ and $\mathbf{r}_j^B$. The expression of Eq. (5) can be also extended to atom-centered multipole interactions.[39]

According to Eq. (5), let us consider the electronic coupling. As mentioned in the Introduction, the TrESP method is developed for the electronic coupling calculations. In this method, the electronic coupling is evaluated as the classical

This article is copyrighted as indicated in the article. Reuse of AIP content is subject to the terms at: http://scitation.aip.org/termsconditions. Downloaded to IP: 133.30.52.204 On: Thu, 04 Dec 2014 05:09:54

Coulomb interactions between atomic transition-charges[16]

$$V_{\mathrm{Coul}}^{\mathrm{TrESP\text{-}C}} = \sum_{i\in A}\sum_{j\in B}\frac{q_i q_j}{R_{ij}}, \tag{7}$$

where q_k denotes the transition charge for atom k ($k = i$ or j) in the molecule X. It is noted that Eq. (7) has a double summation in terms of the atom i in the molecule A and the atom j in the molecule B, because of the atomic charge interactions. As mentioned in Sec. II A, the electronic coupling has a similar form to the intermolecular electrostatic energy. Taking into account this similarity, the electronic coupling given by Eq. (7) is expected to be modified by adding the higher order multipole interactions, such as Eq. (5). If the rank of the multipole is taken to be $l = 0$, 1, and 2, the electronic coupling is described as

$$\begin{aligned} V_{\mathrm{Coul}}^{\mathrm{TrESP\text{-}CDQ}} = \sum_{i\in A}\sum_{j\in B}\Bigg[& T_{ij}q_i q_j + \sum_{\alpha} T_{ij,\alpha}(q_i\mu_{j,\alpha} - \mu_{i,\alpha}q_j) \\ & + \frac{1}{3}\sum_{\alpha,\beta} T_{ij,\alpha\beta}(q_i\theta_{j,\alpha\beta} + \theta_{i,\alpha\beta}q_j - 3\mu_{i,\alpha}\mu_{j,\beta}) \\ & + \frac{1}{3}\sum_{\alpha,\beta,\gamma} T_{ij,\alpha\beta\gamma}(\theta_{i,\alpha\beta}\mu_{j,\gamma} - \mu_{i,\alpha}\theta_{j,\beta\gamma}) \\ & + \frac{1}{9}\sum_{\alpha,\beta,\gamma,\delta} T_{ij,\alpha\beta\gamma\delta}\theta_{i,\alpha\beta}\theta_{j,\gamma\delta}\Bigg], \end{aligned} \tag{8}$$

where $\mu_{k,\alpha}$ and $\theta_{k,\alpha\beta}$ denote an α component of a transition dipole for the atom k and an $\alpha\beta$ component of a transition quadrupole for the atom k, respectively. These moments are defined by

$$\boldsymbol{\mu}_k \equiv q_k\mathbf{r}_k = q_k(x_k, y_k, z_k), \tag{9a}$$

$$\boldsymbol{\theta}_k \equiv \frac{1}{2}q_k\begin{pmatrix} 3x_k^2 - r_k^2 & 3x_k y_k & 3x_k z_k \\ 3y_k x_k & 3y_k^2 - r_k^2 & 3y_k z_k \\ 3z_k x_k & 3z_k y_k & 3z_k^2 - r_k^2 \end{pmatrix}, \tag{9b}$$

where $\mathbf{r}_k$ denotes a position vector of the atom k, and x_k, y_k, and z_k express its components. The distance of $\mathbf{r}_k$ is given by r_k, so that r_k^2 corresponds to $r_k^2 = x_k^2 + y_k^2 + z_k^2$. The tensors $T_{ij,\alpha\cdots}$ in Eq. (8) are explicitly written as

$$T_{ij,\alpha} = -R_{ij,\alpha}R_{ij}^{-3}, \tag{10a}$$

$$T_{ij,\alpha\beta} = 3R_{ij,\alpha}R_{ij,\beta}R_{ij}^{-5} - \delta_{\alpha\beta}R_{ij}^{-3}, \tag{10b}$$

$$\begin{aligned} T_{ij,\alpha\beta\gamma} = & -15R_{ij,\alpha}R_{ij,\beta}R_{ij,\gamma}R_{ij}^{-7} \\ & +3\left(R_{ij,\alpha}\delta_{\beta\gamma} + R_{ij,\beta}\delta_{\alpha\gamma} + R_{ij,\gamma}\delta_{\alpha\beta}\right)R_{ij}^{-5}, \end{aligned} \tag{10c}$$

$$\begin{aligned} T_{ij,\alpha\beta\gamma\delta} = & 105R_{ij,\alpha}R_{ij,\beta}R_{ij,\gamma}R_{ij,\delta}R_{ij}^{-9} - 15(R_{ij,\alpha}R_{ij,\beta}\delta_{\gamma\delta} \\ & + R_{ij,\gamma}R_{ij,\delta}\delta_{\alpha\beta} + R_{ij,\beta}R_{ij,\delta}\delta_{\alpha\gamma} + R_{ij,\beta}R_{ij,\gamma}\delta_{\alpha\delta} \\ & + R_{ij,\alpha}R_{ij,\gamma}\delta_{\beta\delta} + R_{ij,\alpha}R_{ij,\delta}\delta_{\beta\gamma})R_{ij}^{-7} \\ & + 3(\delta_{\alpha\beta}\delta_{\gamma\delta} + \delta_{\alpha\gamma}\delta_{\beta\delta} + \delta_{\alpha\delta}\delta_{\beta\gamma})R_{ij}^{-5}, \end{aligned} \tag{10d}$$

where $\delta_{\alpha\beta}$ represents Kronecker delta. Equation (8) is the TrESP-CDQ expression of the electronic coupling. Compared with the original TrESP method (Eq. (7)), the TrESP-CDQ method includes not only the charge-charge interaction but also the charge-dipole, charge-quadrupole, dipole-dipole, dipole-quadrupole, and quadrupole-quadrupole interactions.

C. Determinations of the transition charges, dipoles, and quadrupoles

The electronic coupling calculation based on Eq. (8) requires the transition charges, dipoles, and quadrupoles for the kth atom in the molecule X. In this study, these values are determined from the ESP fitting procedure.[31,32]

Let us consider the following function for a least square fitting:

$$Z = \sum_{a}^{m}\left(v_a^{\mathrm{CL}} - v_a^{\mathrm{QM}}\right)^2 + \lambda\left(\sum_{k}^{n} q_k - q_{\mathrm{Tot}}\right), \tag{11}$$

where v_a^{CL} and v_a^{QM} denote classically and quantum-mechanically calculated ESPs at point a, respectively. The numbers of the ESP points and of the atoms in the molecule X are expressed as m and n, respectively. Using Eqs. (10a) and (10b), the classical ESP v_a^{CL} is described as

$$v_a^{\mathrm{CL}} = \sum_{k}^{n}\left(T_{ak}q_k - \sum_{\alpha} T_{ak,\alpha}\mu_{k,\alpha} + \frac{1}{3}\sum_{\alpha,\beta} T_{ak,\alpha\beta}\theta_{k,\alpha\beta}\right). \tag{12}$$

The first, second, and third terms in Eq. (12) correspond to the contributions from the transition charges, dipoles, and quadrupoles, respectively. In the original TrESP method,[16] only the first term is concerned for this potential.[27] In Eq. (11), the quantum-mechanical ESP v_a^{QM} corresponds to the reference value for the fitting. This potential is calculated with the transition density

$$\begin{aligned} v_a^{\mathrm{QM}} &= -\int \mathrm{d}\mathbf{r}_1 \frac{\rho_{p0}^X(\mathbf{r}_1)}{|\mathbf{r}_a - \mathbf{r}_1|} \\ &= -\sum_{\mu,\nu\in X}\left(P_{p0}^X\right)_{\nu\mu}\int \mathrm{d}\mathbf{r}_1 \frac{\chi_\mu{}^*(\mathbf{r}_1)\chi_\nu(\mathbf{r}_1)}{|\mathbf{r}_a - \mathbf{r}_1|}, \end{aligned} \tag{13}$$

where $\chi_\nu(\mathbf{r}_1)$ denotes an atomic orbital (AO), and $\int \mathrm{d}\mathbf{r}_1 \chi_\mu{}^*(\mathbf{r}_1)\chi_\nu(\mathbf{r}_1)/|\mathbf{r}_a - \mathbf{r}_1|$ is a one-electron integral in the AO representation. In the second line of Eq. (13), the transition density is converted to the matrix form $(P_{p0}^X)_{\nu\mu}$, which is defined by

$$\left(P_{p0}^X\right)_{\nu\mu} \equiv \int \mathrm{d}\mathbf{r}_1 \chi_\nu^*(\mathbf{r}_1)\rho_{p0}^X(\mathbf{r}_1)\chi_\mu(\mathbf{r}_1). \tag{14}$$

It is noted that the present approach employs the self-consistent transition density matrix as $(P_{p0}^X)_{\nu\mu}$, although the original TrESP method uses the transition density matrix obtained from the isolated monomer calculation. The self-consistent transition density matrix is obtained with a density-fragment interaction (DFI) method.[30] It is also noted that Eq. (13) is the ESP of the transition density. This potential

This article is copyrighted as indicated in the article. Reuse of AIP content is subject to the terms at: http://scitation.aip.org/termsconditions. Downloaded to IP: 133.30.52.204 On: Thu, 04 Dec 2014 05:09:54

is different from the ESP of the ground state density, which is used in the standard ESP fitting procedure.[31] In the case of $p = 0$, Eq. (13) corresponds to the ESP of the ground state density. In Eq. (11), q_{Tot} denotes total transition-charge of the molecule X and λ is Lagrange multiplier for the constraint of the transition charges. The total transition-charge must be taken to be zero because of the orthogonality between the ground state and the pth excited state,

$$q_{\mathrm{Tot}} = \int \mathrm{d}\mathbf{r}_1 \rho^X_{p0}(\mathbf{r}_1) = 0. \tag{15}$$

For $p = 0$, this value becomes the number of electrons for the molecule X, N_{e}^X. It is noted that the nuclear contributions to the ESPs and to the total transition-charge are not included in Eq. (11) also due to the orthogonality. This point is also different from the standard ESP fitting.

To find the minimum of Eq. (11), we next consider grad$Z$ = 0, i.e.,

$$\frac{\partial Z}{\partial q_l} = \frac{\partial Z}{\partial \mu_{l,\alpha}} = \frac{\partial Z}{\partial \theta_{l,\alpha\beta}} = 0, \tag{16a}$$

and the constraint imposed on the transition charges,

$$\sum_k^n q_k - q_{\mathrm{Tot}} = 0. \tag{16b}$$

In Eq. (16a), $l = 1, 2, \cdots n$, and the Greek letters (α and β) represent the components of Eqs. (9a) and (9b). Then Eqs. (16a) and (16b) yield a $(13n + 1) \times (13n + 1)$ system of equations, which is written as

$$\begin{pmatrix} \mathbf{A}^{\mathrm{I}} & \mathbf{A}^{\mathrm{II}} & \mathbf{A}^{\mathrm{III}} & \mathbf{I} \\ \mathbf{A}^{\mathrm{II}T} & \mathbf{A}^{\mathrm{IV}} & \mathbf{A}^{\mathrm{V}} & \mathbf{0} \\ \mathbf{A}^{\mathrm{III}T} & \mathbf{A}^{\mathrm{V}T} & \mathbf{A}^{\mathrm{VI}} & \mathbf{0} \\ \mathbf{I}^T & \mathbf{0} & \mathbf{0} & \mathbf{0} \end{pmatrix} \begin{pmatrix} \mathbf{q} \\ \boldsymbol{\mu} \\ \boldsymbol{\theta} \\ \lambda \end{pmatrix} = \begin{pmatrix} \mathbf{B}^{\mathrm{I}} \\ \mathbf{B}^{\mathrm{II}} \\ \mathbf{B}^{\mathrm{III}} \\ q_{\mathrm{Tot}} \end{pmatrix}. \tag{17}$$

This is the matrix equation, $\mathbf{AM} = \mathbf{B}$. The matrix $\mathbf{A}$ is composed of the submatrices $\mathbf{A}^{\mathrm{I}}$, $\mathbf{A}^{\mathrm{II}}$, $\mathbf{A}^{\mathrm{III}}$, $\mathbf{A}^{\mathrm{IV}}$, $\mathbf{A}^{\mathrm{V}}$, $\mathbf{A}^{\mathrm{VI}}$, $\mathbf{0}$, and $\mathbf{I}$. The superscript T denotes a transpose. These submatrices are expressed as follows:

$$A^{\mathrm{I}}_{kl} = \sum_a^m \frac{1}{R_{ak} R_{al}}, \tag{18a}$$

$$A^{\mathrm{II}}_{kl,\alpha} = \sum_a^m \frac{R_{al,\alpha}}{R_{ak} R^3_{al}}, \tag{18b}$$

$$A^{\mathrm{III}}_{kl,\alpha\beta} = \sum_a^m \frac{R_{al,\alpha} R_{al,\beta} - \delta_{\alpha\beta} R^2_{al}/3}{R_{ak} R^5_{al}}, \tag{18c}$$

$$A^{\mathrm{IV}}_{kl,\alpha\beta} = \sum_a^m \frac{R_{ak,\alpha} R_{al,\beta}}{R^3_{ak} R^3_{al}}, \tag{18d}$$

$$A^{\mathrm{V}}_{kl,\alpha\beta\gamma} = \sum_a^m \frac{R_{ak,\alpha} \left(R_{al,\beta} R_{al,\gamma} - \delta_{\beta\gamma} R^2_{al}/3\right)}{R^3_{ak} R^5_{al}}, \tag{18e}$$

$$A^{\mathrm{VI}}_{kl,\alpha\beta\gamma\delta} = \sum_a^m \frac{\left(R_{ak,\alpha} R_{ak,\beta} - \delta_{\alpha\beta} R^2_{ak}/3\right) \left(R_{al,\gamma} R_{al,\delta} - \delta_{\gamma\delta} R^2_{al}/3\right)}{R^5_{ak} R^5_{al}}. \tag{18f}$$

The submatrices $\mathbf{A}^{\mathrm{I}}$, $\mathbf{A}^{\mathrm{II}}$, $\mathbf{A}^{\mathrm{III}}$, $\mathbf{A}^{\mathrm{IV}}$, $\mathbf{A}^{\mathrm{V}}$, and $\mathbf{A}^{\mathrm{VI}}$ are $n \times n$, $n \times 3n$, $n \times 9n$, $3n \times 3n$, $3n \times 9n$, and $9n \times 9n$ matrices, respectively. The submatrix $\mathbf{0}$ expresses the zero matrix, and $\mathbf{I}$ is given by

$$\mathbf{I} = \underbrace{(1, 1, \cdots, 1)^T}_{n}. \tag{19}$$

All of n elements in this submatrix are 1. The submatrices in $\mathbf{B}$ are given by

$$B^{\mathrm{I}}_l = \sum_a^m \frac{V^{\mathrm{QM}}_a}{R_{al}}, \tag{20a}$$

$$B^{\mathrm{II}}_{l,\alpha} = \sum_a^m \frac{V^{\mathrm{QM}}_a R_{al,\alpha}}{R^3_{al}}, \tag{20b}$$

$$B^{\mathrm{III}}_{l,\alpha\beta} = \sum_a^m \frac{V^{\mathrm{QM}}_a (R_{al,\alpha} R_{al,\beta} - \delta_{\alpha\beta} R^2_{al}/3)}{R^5_{al}}. \tag{20c}$$

The submatrices $\mathbf{B}^{\mathrm{I}}$, $\mathbf{B}^{\mathrm{II}}$, and $\mathbf{B}^{\mathrm{III}}$ are $n \times 1$, $3n \times 1$, and $9n \times 1$ matrices, respectively. As shown in Eq. (15), q_{Tot} in the matrix $\mathbf{B}$ is set to be zero. The submatrices $\mathbf{q}$, $\boldsymbol{\mu}$, and $\boldsymbol{\theta}$ in the matrix $\mathbf{M}$ contain the transition charges, dipoles, and quadrupoles for the individual atoms, so that they have n, $3n$, and $9n$ elements, respectively,

$$\mathbf{q} = \underbrace{(q_1, q_2, \cdots q_n)^T}_{n}, \tag{21a}$$

$$\boldsymbol{\mu} = \underbrace{(\mu_{1,x}, \mu_{1,y}, \cdots, \mu_{n,z})^T}_{3n}, \tag{21b}$$

$$\boldsymbol{\theta} = \underbrace{(\theta_{1,xx}, \theta_{1,xy}, \cdots, \theta_{n,zz})^T}_{9n}. \tag{21c}$$

For the determinations of $\mathbf{q}$, $\boldsymbol{\mu}$, and $\boldsymbol{\theta}$, Eq. (17) is solved with the inverse matrix of $\mathbf{A}$. This procedure is performed with singular value decomposition (SVD).[32] Finally, the TrESP-CDQ calculation based on Eq. (8) is performed with the obtained values of $\mathbf{q}$, $\boldsymbol{\mu}$, and $\boldsymbol{\theta}$.

III. COMPUTATIONAL DETAILS

In this study, a helium dimer, a methane dimer, and an ethylene dimer were selected as computational models. The atomic coordinates of these models were obtained from the geometry optimization using the coupled-cluster with single, double, and perturbative triple excitations (CCSD(T)) method.[41] For the methane dimer and the ethylene dimer, the structures in S22 database[40] were referenced. In the calculations of the helium dimer, Dunning's augmented correlation consistent basis set (aug-cc-pVQZ)[42] was used. In the calculations of the methane dimer and the ethylene dimer, Dunning's

This article is copyrighted as indicated in the article. Reuse of AIP content is subject to the terms at: http://scitation.aip.org/termsconditions. Downloaded to IP: 133.30.52.204 On: Thu, 04 Dec 2014 05:09:54

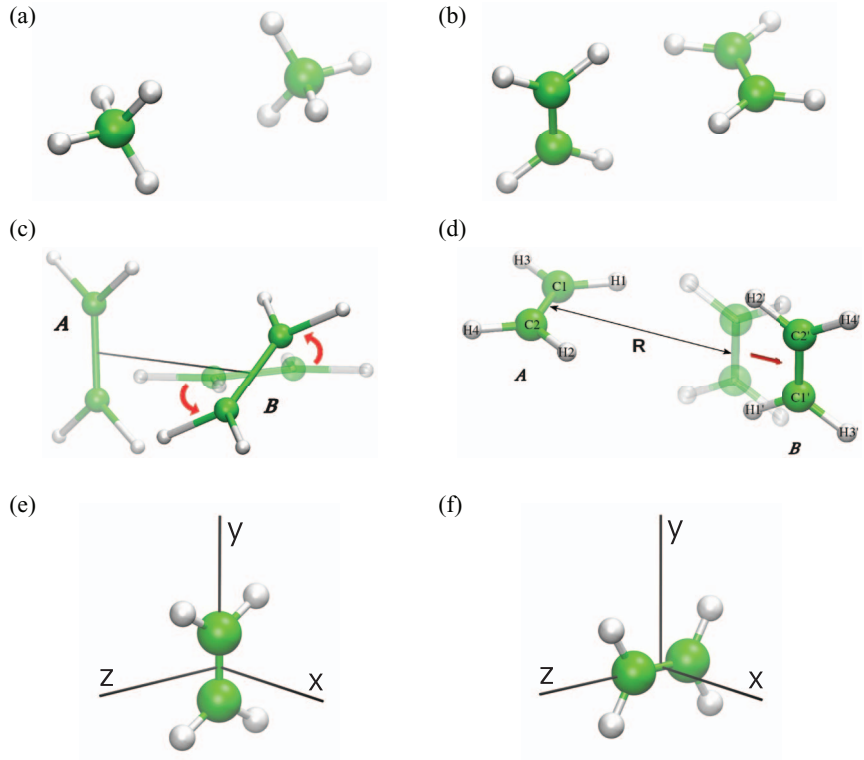

FIG. 1. Optimized structures of (a) the methane dimer and (b) the ethylene dimer. (c) Rotated structure of the ethylene dimer. The ethylene *B* is rotated by 45.0° along the axis of the center-to-center distance. (d) The definition of *x*-axis coordinate for Fig. 2 and the labels of the atoms for Table III are shown. Cartesian coordinates used for the assignments of the symmetry labels of (e) the C_{2v} ethylene and (f) the D_{2h} ethylene.

correlation consistent basis set (cc-pVTZ)[43] was used. These calculations were performed with the Gaussian03 program package.[44] The optimized structures of the methane dimer and the ethylene dimer are illustrated in Fig. 1. The structures of the methane dimer and the ethylene dimer have D_{3d} and D_{2d} symmetry, respectively. The individual methane monomers have C_{3v} symmetry and the ethylene monomers have C_{2v} symmetry. The TrESP-CDQ and TDFI methods were applied to these computational models for calculating the electronic coupling energies.

In the excited state calculations, time-dependent density functional theory (TD-DFT)[45,46] and the configuration interaction singles (CIS)[47] method were employed for obtaining the transition densities. In this process, the DFI method[30] was used to satisfy the self-consistency condition between interfragment interactions. The DFI calculations were iteratively performed until the change in the total energy was converged below a threshold of 1×10^{-5} au. In the TD-DFT calculations, the revised Coulomb-attenuating method (rCAM) B3LYP functional[48] was used. The aug-cc-pVQZ basis set was used for the helium dimer and the cc-pVTZ basis set was used for the methane dimer and the ethylene dimer.

The TrESP-CDQ program for the electronic coupling calculations was implemented in Gaussian03.[44] All of the electronic coupling calculations were performed with Gaussian03, in which the same global Cartesian system was used. Therefore, the input coordinates for the molecular systems (also for the isolated monomers and the finite-separation dimers) were kept during the electronic coupling calculations including the ESP fitting.

IV. RESULTS

A. Accuracy of the TrESP-CDQ method

The accuracy of the TrESP-CDQ method was tested. In the first step, the helium dimer was used as the computational model. To estimate the error associated with the TrESP-CDQ method, the TDFI calculation was also performed, which was used as a reference value. In these calculations, the TD-rCAM-B3LYP and CIS methods were employed to check the dependence on the electronic structure method. The electronic coupling between the fourth excited states for both helium atoms is concerned here because the combination of these states provided the largest value of the electronic coupling energy. The fourth excited state was the 1s → 2p transition with the excitation energy of 22.65 eV for TD-rCAM-B3LYP and of 24.86 eV for CIS, and the oscillator strength was to be 0.272 au for TD-rCAM-B3LYP and 0.289 au for CIS. The orientation of this excited state (2p orbital) was parallel to the axis of the He-He separation. The calculated results are summarized in Table I. The electronic coupling energies obtained with the TrESP-CDQ method were to be 1179.6 cm^{-1} for TD-rCAM-B3LYP and 1143.7 cm^{-1} for CIS, while the TDFI values were to be 1105.7 cm^{-1} and 1088.6 cm^{-1} for TD-rCAM-B3LYP and CIS, respectively. These results showed that the TrESP-CDQ calculations with TD-rCAM-B3LYP and CIS successfully reproduced the reference values with the deviations of 73.9 cm^{-1} and 53.3 cm^{-1}, respectively. Hence, the dependence on the electronic structure method was found to be small from these calculations (37.7 cm^{-1} for TrESP-CDQ and 17.1 cm^{-1} for TDFI). To evaluate the effects of the

This article is copyrighted as indicated in the article. Reuse of AIP content is subject to the terms at: http://scitation.aip.org/termsconditions. Downloaded to IP: 133.30.52.204 On: Thu, 04 Dec 2014 05:09:54

TABLE I. Electronic coupling energies of the helium dimer (cm^{-1}).[a]

	TrESP		
	CD	CDQ	TDFI
TD-rCAM-B3LYP	1181.8	1179.6	1105.7
CIS	1143.7	1141.9	1088.6

[a]Combination of the fourth excited states for both helium atoms was considered. The fourth excited state was the 1s → 2p transition.

transition dipoles and quadrupoles, the TrESP calculations with the transition charges and dipoles (TrESP-CD) were also performed. As listed in Table I, the TrESP-CD values were to be 1181.8 cm^{-1} for TD-rCAM-B3LYP and 1143.7 cm^{-1} for CIS, which reproduced the reference values with the deviations of 76.1 cm^{-1} and 55.1 cm^{-1} for TD-rCAM-B3LYP and CIS, respectively. Hence, the TrESP-CD values became almost the same as the TrESP-CDQ ones. The deviations from the TrESP-CDQ values were to be 2.2 cm^{-1} and 1.8 cm^{-1} for TD-rCAM-B3LYP and CIS, respectively. In the case of only one atom, the first nonzero order in the spherical harmonic expansion in a transition density becomes a dipole. Therefore, the transition dipole interaction mainly contributed to the electronic coupling energy for this system.

Next, the TrESP-CDQ method was applied to the methane dimer. These calculations were performed with TD-rCAM-B3LYP. The first three excited states for the methane monomer were concerned here, and the electronic coupling energies between the same excited states for both methane molecules were calculated. The first excited state showed the excitation energy of 11.21 eV with the oscillator strength of 0.l66 au, and it had the symmetry of the A_1 irreducible representation. The rest two excited states were degenerate, which showed the excitation energy of 11.27 eV with the oscillator strength of 0.186 au. Both the excited states had the symmetry of the E irreducible representation. These three excited states were characterized as the σ-σ^* excitations. The orientation of the first excited state (HOMO → LUMO transition) was parallel to the axis of the C-C separation, while the doubly degenerate excited states (HOMO–1 → LUMO transition and HOMO–2 → LUMO transition) were oriented perpendicularly to the axis of the C-C separation. The calculated electronic coupling energies are summarized in Table II. The combination of the first excited states for both methane molecules is abbreviated as (1,1) and that of the second excited states is as (2,2). Since the second excited state was doubly degenerate, the calculated electronic coupling energies became the same values. The TrESP-CDQ method gave the electronic coupling energies of 260.3 cm^{-1} for (1,1) and 439.8 cm^{-1} for (2,2), which successfully reproduced the reference values (241.6 cm^{-1} and 431.0 cm^{-1}) with the deviations of 18.7 cm^{-1} and 8.8 cm^{-1}. The TrESP-CD and TrESP-C calculations were also performed to the methane dimer, which led to the electronic coupling energies of 263.2 cm^{-1} and 276.8 cm^{-1} for (1,1) and 440.7 cm^{-1} and 487.2 cm^{-1} for (2,2). The deviations from the reference value were to be 21.6 cm^{-1} and 9.7 cm^{-1} for TrESP-CD and to be 35.2 cm^{-1} and 56.2 cm^{-1} for TrESP-C. From these results, the TrESP-CDQ and TrESP-CD methods were found to give a quantitative description of the electronic coupling energy. Although the TrESP-C method was not applicable to the helium dimer, it worked well for the methane dimer. Similar calculations were performed to the ethylene dimer. These calculations were also performed with TD-rCAM-B3LYP. The electronic coupling between the first and second excited state transition densities was concerned for these calculations. Figure 1(e) shows the definition of Cartesian coordinates used for the assignment of the symmetry labels for the ethylene monomer. The principal axis (C_2 rotational axis) is set to the z-axis. The first excited state (HOMO → LUMO transition) was characterized as the π-π^* excitation, which had the symmetry of the B_2 irreducible representation. On the other hand, the second excited state (HOMO–1 → LUMO transition) was to be the σ-π^* excitation and it had the symmetry of the B_1 irreducible representation. The first and second excited states showed the excitation energies of 7.80 eV and 8.18 eV, respectively. The oscillator strength was to be 0.361 au and 0.001 au for the first and second excited states, respectively. The ethylene dimer shown in Fig. 1(b) has the center-to-center distance of 3.72 Å. The torsion angle between the molecular planes of the two etylenes is 90.0°. The calculated electronic coupling energies are also summarized in Table II. As found here, the TrESP-CDQ method (251.5 cm^{-1}) successfully reproduced the

TABLE II. Electronic coupling energies of the methane dimer and the ethylene dimer (cm^{-1}).[a]

		TrESP			
	Excited states[b]	C	CD	CDQ	TDFI
Methane dimer	(1,1)[c]	276.8	263.2	260.3 (332.1)[d]	241.6 (289.4)[d]
	(2,2)[e]	487.2	440.7	439.8 (499.7)[d]	431.0 (484.0)[d]
Ethylene dimer	(1,2)[f]	1.97×10^{-2}	297.5	251.5 (482.4)[d]	251.7 (459.7)[d]
Ethylene dimer (45°)[g]	(1,2)[f]	12.5	167.2	139.6 (339.5)[d]	136.1 (315.7)[d]

[a]All calculations were performed with TD-rCAM-B3LYP/cc-pVTZ.
[b]Combinations of the excited states for monomers.
[c]The first excited state was the σ-σ^* excitation and had the A_1 symmetry.
[d]Transition densities obtained from isolated monomer calculations were used.
[e]The second excited state was the σ-σ^* excitation and had the E symmetry.
[f]The first excited state was the π-π^* excitation and had the B_2 symmetry. The second excited state was the σ-π^* excitation and had the B_1 symmetry.
[g]The ethylene B was rotated by 45° along the axis of the center-to-center distance.

This article is copyrighted as indicated in the article. Reuse of AIP content is subject to the terms at: http://scitation.aip.org/termsconditions. Downloaded to IP: 133.30.52.204 On: Thu, 04 Dec 2014 05:09:54

reference value (251.7 cm^{-1}) with the deviation of 0.2 cm^{-1}. The TrESP-CD method (297.5 cm^{-1}) also reproduced the reference value with the deviation of 45.8 cm^{-1}. In contrast, the TrESP-C method (1.97×10^{-2} cm^{-1}) completely failed in describing the reference value. The electronic coupling calculations were performed to a different geometry shown in Fig. 1(c). This geometry was obtained by rotating the ethylene *B* by 45.0° along the axis of the center-to-center distance. The combination of the first and second excited states was considered for the electronic coupling calculations. The first excited state showed the excitation energy of 7.81 eV with the oscillator strength of 0.361 au. The second excited state showed the excitation energy of 8.17 eV with the oscillator strength of 0.001 au. The characters of the individual excited states were the same as those of the optimized geometry. The calculated electronic coupling energies are also listed in Table II. The TrESP-CDQ method (139.6 cm^{-1}) successfully reproduced the reference value (136.1 cm^{-1}) with the deviation of 3.5 cm^{-1}. The TrESP-CD method (167.2 cm^{-1}) also reproduced the reference value with the deviation of 31.1 cm^{-1}. The TrESP-C method gave the electronic coupling energy of 12.5 cm^{-1}, which completely failed in describing the reference value. These results clearly showed that the TrESP-CDQ and TrESP-CD methods gave a much improved description of the electronic coupling energy, compared with the TrESP-C method.

As mentioned in Sec. II C, the self-consistent transition density was employed in the present ESP fitting. To examine this effect, the electronic coupling calculations were performed with transition densities obtained from the isolated monomer calculations. It is noted that the effect of the interfragment interactions is not included in these monomer calculations. This electronic coupling calculation is abbreviated as TrESP0-CDQ. The calculated values are also listed in Table II. In the case of the methane dimer, the electronic coupling energies for TrESP0-CDQ were to be 332.1 cm^{-1} for (1,1) and 499.7 cm^{-1} for (2,2), which were larger by 71.8 cm^{-1} and 59.9 cm^{-1} than the values with the self-consistent densities (260.3 cm^{-1} and 439.8 cm^{-1}). In the case of the ethylene dimer, the TrESP0-CDQ values became 482.4 cm^{-1} for the optimized geometry and 339.5 cm^{-1} for the rotated geometry, which resulted in overestimations of 230.9 cm^{-1} and 199.9 cm^{-1} from the values with the self-consistent densities (251.5 cm^{-1} and 139.6 cm^{-1}). Such a significant difference in the electronic coupling energy was obtained also from the reference values (47.8 cm^{-1} and 53.0 cm^{-1} for the methane dimer and 208.0 cm^{-1} and 179.6 cm^{-1} for the ethylene dimer). These results revealed that the self-consistent transition densities obtained with the DFI method played a significant role in the accurate description of the electronic coupling.

As mentioned in Sec. II A, the overlap between the basis functions is assumed to be small in the present study. To examine this assumption, the overlap between $|\Phi_1\rangle$ and $|\Phi_2\rangle$ (i.e., $\langle\Phi_1|\Phi_2\rangle$) was also calculated. As a result, the values of $\langle\Phi_1|\Phi_2\rangle$ were calculated to be 4.54×10^{-5} and 1.17×10^{-5} for the methane dimer and the ethylene dimer, respectively. These small overlaps indicated that the present assumption was valid for these systems.

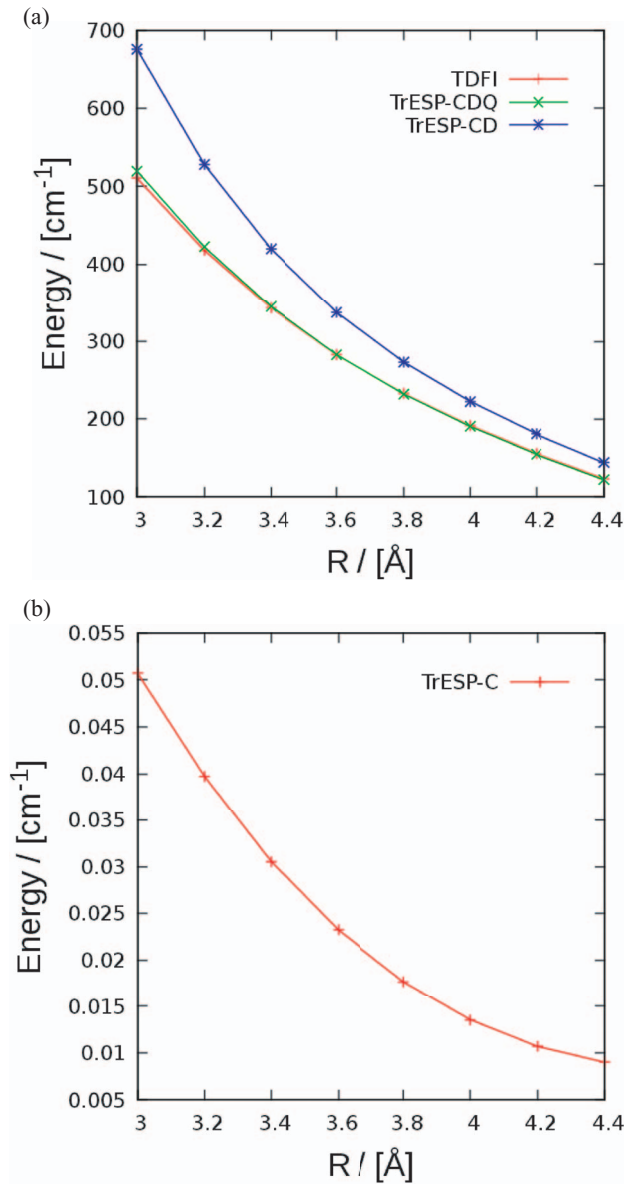

FIG. 2. Electronic coupling energies between two ethylene molecules as a function of intermolecular distance. (a) TDFI, TrESP-CDQ, and TrESP-CD values and (b) TrESP-C values. All calculations are performed with TD-rCAM-B3LYP/cc-pVTZ.

To gain further insight into the accuracy of the TrESP-CDQ method, the dependence on the intermolecular separation was investigated. Figure 2 shows the evolutions of the electronic coupling energies as a function of the intermolecular distance of the ethylene dimer. The definition of the *x*-axis coordinate is shown in Fig. 1(d). The optimized structure corresponds to the intermolecular distance of 3.72 Å. The TrESP-CDQ method gave the electronic coupling energy of 519.5 cm^{-1} at 3.00 Å. This energy gradually became small with the increase in the intermolecular distance. Consequently, the electronic coupling energies obtained with TrESP-CDQ became almost the same as the reference values. The deviations from the reference values were to be ~9.0 cm^{-1}. Figure 2 also shows the electronic coupling energies obtained with the TrESP-CD and TrESP-C methods. As found here, the TrESP-CD values were larger than the

This article is copyrighted as indicated in the article. Reuse of AIP content is subject to the terms at: http://scitation.aip.org/termsconditions. Downloaded to IP: 133.30.52.204 On: Thu, 04 Dec 2014 05:09:54

reference values. At 3.00 Å, the TrESP-CD value was to be 675.7 cm^{-1}, which gave an overestimation of 165.2 cm^{-1} from the reference value. However, the energy curve of TrESP-CD showed a similar shape to the reference values. It gradually became small with the increase in the intermolecular distance. On the other hand, the TrESP-C values were to be almost zero ($\sim$0.05 cm^{-1}) in all the regions calculated. From these results, it was confirmed that the TrESP-CDQ method could quantitatively describe the reference values without respect to the intermolecular separation. These calculations also revealed that the TrESP-C method could not describe the electronic coupling for this system. The overlap $\langle\Phi_1|\Phi_2\rangle$ was also evaluated. As a result, the values of $\langle\Phi_1|\Phi_2\rangle$ were calculated to be 1.07×10^{-4} (3.00 Å) $\sim 2.99 \times 10^{-7}$ (4.40 Å). Although the overlap became large with the decrease in the intermolecular distance, the magnitudes were not large. In the case of large overlap, the indirect coupling is known to give a significant contribution to the amount of electronic coupling.[35,36] However, the present study does not focus on this effect because the TrESP-CDQ method cannot describe the indirect coupling.

B. Analysis of the electronic coupling energy

Based on the successful descriptions of the reference values, the contributions to the electronic coupling energies were analyzed. Table III summarizes the transition charges, dipoles, and quadrupoles for the individual atoms of the optimized ethylene dimer. The labels of the atoms are shown in Fig. 1(d). The magnitudes of the transition dipoles and quadrupoles were given by $|\boldsymbol{\mu}_k| = \sqrt{\sum_\alpha \mu_{k,\alpha}^2}$ and $|\boldsymbol{\theta}_k| = \sqrt{\sum_{\alpha,\beta} \theta_{k,\alpha\beta}^2}$, respectively. As mentioned in Sec. II C, the values of the transition charges, dipoles, and quadrupoles were determined so as to reproduce the quantum-mechanical ESP. Therefore, the constraints to the transition dipoles and quadrupoles were not considered in the present method.

TABLE III. Transition charges, dipoles, and quadrupoles of the ethylene dimer (au).

State[a]	Atom[b]	Charge[c]	Dipole[d]	Quadrupole[e]
1	C1	2.166 (0.829)	0.718	3.730
	C2	− 2.269 (−0.824)	0.670	3.876
	H1	− 0.695 (−0.086)	0.517	0.249
	H2	0.768 (0.083)	0.586	0.295
	H3	− 0.747 (−0.072)	0.539	0.270
	H4	0.777 (0.069)	0.573	0.292
2	C1′	0.027 (0.004)	0.479	1.551
	C2′	− 0.005 (0.003)	0.362	2.211
	H1′	− 0.185 (−0.004)	0.136	0.213
	H2′	0.168 (−0.002)	0.151	0.335
	H3′	0.030 (0.000)	0.176	0.247
	H4′	− 0.034 (−0.002)	0.231	0.336

[a]Data of the 1st and 2nd excited states are shown.
[b]The labels of the atoms are shown in Fig. 1(d).
[c]Data in parentheses were obtained with the ESP fitting only for the transition charges.
[d]The magnitudes of the transition dipoles are shown.
[e]The magnitudes of the transition quadrupoles are shown.

Although the electronic coupling energies were successfully described with the present method, the lack of the constraints may include some symmetry breaking. As found from Table III, the magnitudes of the transition charges of the ethylene *B* were to be quite small, compared with those of the ethylene *A*. While the ethylene *A* had the transition charges of 2.166 au for the C1 atom and −2.269 au for the C2 atom, the transition charges for the atoms C1′ and C2′ of the ethylene *B* were to be 0.027 au and −0.005 au, respectively. These results indicated a negligible contribution of the transition charge interactions to the electronic coupling. Table III also lists the transition charges used in the TrESP-C method. These values were determined from the ESP fitting only for the transition charges. In this case, the transition charges of the ethylene *B* became almost zero (−0.004 to 0.004 au). As mentioned in Sec. IV A, the electronic coupling obtained with the TrESP-C method became almost zero. It was caused by almost zero values of the transition charges for the ethylene *B*. On the other hand, the magnitudes of the transition dipoles and quadrupoles for the ethylene *B* were to be 0.136–0.479 au and 0.213–2.211 au, respectively. For the atoms C1′ and C2′, the transition dipoles were to be 0.479 au and 0.362 au, and the transition quadurupoles were to be 1.551 au and 2.211 au. These transition dipoles had more than half of the values for the ethylene *A* (0.718 au for C1 and 0.670 au for C2). From these results, the transition dipoles and quadrupoles for the ethylene *B* were found to be large, compared with the transition charges. Owing to these transition dipoles and quadrupoles, the TrESP-CDQ method could quantitatively describe the electronic coupling energy.

The magnitudes of the transition charges, dipoles, and quadrupoles are strongly related to the characters of the excited states. As mentioned in Sec. IV A, the first and second excited states of the ethylene monomer had the oscillator strength of 0.361 au and 0.001 au, respectively. This means an allowed transition for the first excited state and almost a forbidden transition for the second excited state. These characters are understood from the transition densities. Figure 3(a) illustrates the transition densities of the optimized ethylene dimer. The positive and negative phases of the transition densities are represented by red and blue colors, respectively. Since the first (B_2 symmetry) and second (B_1 symmetry) excited states were considered in the present system, the transition densities of the individual ethylenes formed different shapes. For example, the transition density of the ethylene *A* (the first excited state) was to be anti-symmetric between the atoms C1 and C2, while that of the ethylene *B* (the second excited state) was to be symmetric between the atoms C1′ and C2′. Alternatively, the transition density of the ethylene *A* was to be symmetric to the mirror plane corresponding to the molecular plane for the ethylene *A*, while that of the ethylene *B* was to be anti-symmetric to the corresponding mirror plane. Although each ethylene molecule in this system has the C_{2v} symmetry, this molecular structure is similar to the D_{2h} symmetry. In the case of the D_{2h} symmetry, the similar characters to the first and second excited states were obtained from the B_{1u} and B_{1g} states, respectively. These symmetry labels were assigned from Cartesian coordinates illustrated in Fig. 1(f) where the principal axis is set to the *z*-axis.

This article is copyrighted as indicated in the article. Reuse of AIP content is subject to the terms at: http://scitation.aip.org/termsconditions. Downloaded to IP: 133.30.52.204 On: Thu, 04 Dec 2014 05:09:54

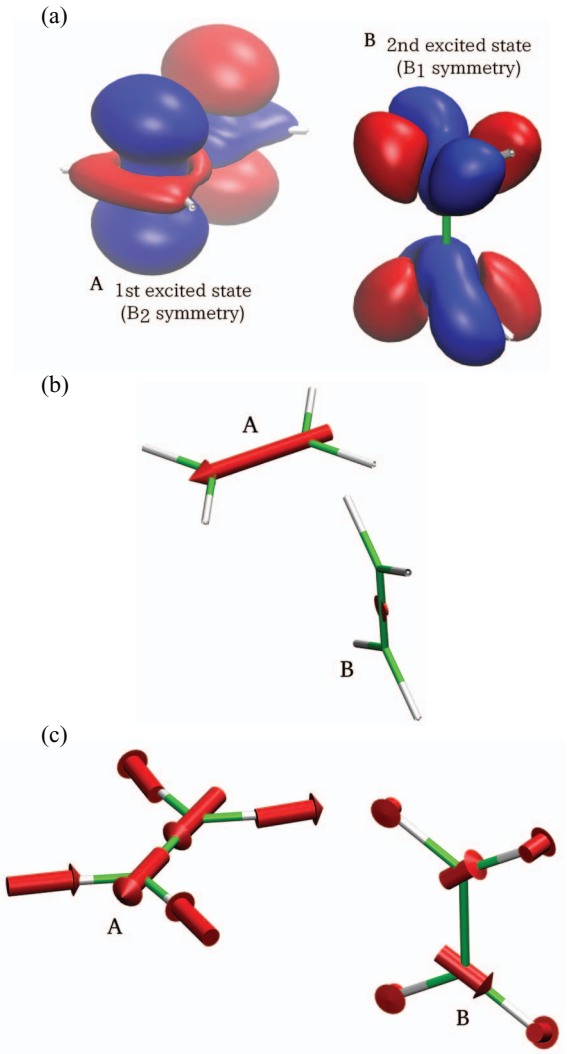

FIG. 3. (a) Transition density distributions, (b) molecular transition dipole moments, and (c) atomic transition dipole moments. In (a), the isovalues of 0.01 electrons/Å^3 and −0.01 electrons/Å^3 are represented by red and blue colors, respectively. The ethylene *A* shows the first excited state (the π-π^* excitation) and it had the B_2 symmetry. The ethylene *B* shows the second excited state (the σ-π^* excitation) and it had the B_1 symmetry.

According to the selection rule, the B_{1u} and B_{1g} states correspond to the allowed and forbidden transitions, respectively. Therefore, these transition densities made a significant difference in the molecular transition dipole moment. Figure 3(b) shows the molecular transition dipoles for the two ethylenes. Each dipole is represented by a point vector located on the molecular center defined by the center of mass. The dipole-dipole orientation factor was to be 1.00. The molecular transition dipole of the ethylene *B* became quite small (0.048 au), compared with that of the ethylene *A* (1.375 au). In this way, the forbidden transition density cannot be represented by the molecular transition dipole. Similarly, the transition charges cannot represent the distribution of the forbidden transition density, so that the magnitudes of the transition charges for the ethylene *B* became quite small. In other words, the TrESP-C method gives small transition charges for the forbidden transition. On the other hand, the magnitudes of the atomic transition dipoles for the ethylene *B* were to be 0.136–0.479 au, which were much larger than the molecular transition dipole for the ethylene *B* (0.048 au). The atomic transition dipoles for the ethylene dimer were also illustrated in Fig. 3(c). As found here, the individual directions of the atomic transition dipoles provided detailed information on the transition density distributions. In this way, the atomic transition dipoles can represent the distribution of the transition density without respect to the character of the excited state, which can give a contribution to the electronic coupling energy.

V. CONCLUSIONS

In this paper, the TrESP-CDQ approach for the electronic coupling calculations was proposed. The TrESP method is based on the classical description of the electronic Coulomb coupling between interacting molecules. Although only the transition charge interactions were considered in the original TrESP method, the present approach included the contributions from the transition dipoles and quadrupoles as well as the transition charges. Hence, the self-consistent transition density was employed in the ESP fitting procedure. The TrESP-CDQ method was applied to the helium dimer, the methane dimer, and the ethylene dimer. As a result, it succeeded in quantitatively estimating the reference values obtained with the TDFI method. These calculations also showed that the TrESP-CDQ method gave a much improved description of the electronic coupling, compared with the TrESP-C method.

In this study, the effect of the self-consistent transition densities was examined. For this purpose, the electronic coupling calculations were performed with the transition densities that were obtained from the isolated monomer calculations (TrESP0-CDQ). The calculated electronic coupling energies considerably overestimated the values with the self-consistent transition densities. In the TrESP-CDQ method, the self-consistency condition between the interacting molecules was satisfied by the DFI method. Therefore, the DFI method was found to play a significant role in the accuracy of the electronic coupling calculations.

The analysis of the electronic coupling energy was also performed. The TrESP-C method could not describe the electronic coupling energy of the ethylene dimer, which was caused by the almost zero values of the transition charges for the ethylene *B*. On the other hand, the transition dipoles and quadrupoles for the ethylene *B* showed much larger values than the transition charges. Owing to these values, the TrESP-CDQ method successfully described the electronic coupling energy. The present analysis also clarified that the transition density distribution strongly influenced the magnitudes of the transition charges, dipoles, and quadrupoles.

The TrESP-CDQ method can give quantitative descriptions of the electronic Coulomb coupling. This accuracy is almost the same as the TDFI method. In addition, TrESP-CDQ can reduce the computational cost compared with TDFI, so that it is expected to be applied to large molecules. The TrESP-CDQ calculation can be combined with other electronic structure methods, even though only the TD-rCAM-B3LYP and CIS methods were adopted in the present study. Hence, the present approach allows us to estimate the

This article is copyrighted as indicated in the article. Reuse of AIP content is subject to the terms at: http://scitation.aip.org/termsconditions. Downloaded to IP: 133.30.52.204 On: Thu, 04 Dec 2014 05:09:54

contributions to the electronic coupling in terms of the transition charges, dipoles, and quadrupoles. Such estimations cannot be performed with the TDFI method. These advantages of TrESP-CDQ are expected to be useful for analyzing and understanding the mechanism of EET.

ACKNOWLEDGMENTS

This study was supported by JSPS KAKENHI Grant No. 25810004.

[1] V. May and O. Kühn, *Charge and Energy Transfer Dynamics in Molecular Systems*, 3rd ed. (Wiley-VCH, Weinheim, 2011).
[2] G. D. Scholes, Annu. Rev. Phys. Chem. **54**, 57 (2003).
[3] T. Förster, Ann. Phys. **437**, 55 (1948).
[4] J. C. Chang, J. Chem. Phys. **67**, 3901 (1977).
[5] A. Warshel and W. W. Parson, J. Am. Chem. Soc. **109**, 6143 (1987).
[6] H. Nagae, T. Kakitani, T. Katoh, and M. Mimuro, J. Chem. Phys. **98**, 8012 (1993).
[7] G. D. Scholes, K. P. Ghiggino, A. M. Oliver, and M. N. Paddon-Row, J. Phys. Chem. **97**, 11871 (1993).
[8] S. Marguet, D. Markovitsi, P. Millié, and H. Sigal, J. Phys. Chem. B **102**, 4697 (1998).
[9] B. P. Krueger, G. D. Scholes, and G. R. Fleming, J. Phys. Chem. B **102**, 5378 (1998).
[10] A. Damjanović, T. Ritz, and K. Schulten, Phys. Rev. E **59**, 3293 (1999).
[11] D. Beljonne, J. Cornil, R. Silbey, P. Millié, and J. L. Brédas, J. Chem. Phys. **112**, 4749 (2000).
[12] S. Tretiak, C. Middleton, V. Chernyak, and S. Mukamel, J. Phys. Chem. B **104**, 4519 (2000).
[13] C.-P. Hsu, G. R. Fleming, M. Head-Gordon, and T. Head-Gordon, J. Chem. Phys. **114**, 3065 (2001).
[14] M. F. Iozzi, B. Mennucci, J. Tomasi, and R. Cammi, J. Chem. Phys. **120**, 7029 (2004).
[15] K. F. Wong, B. Bagchi, and P. J. Rossky, J. Phys. Chem. A **108**, 5752 (2004).
[16] M. E. Madjet, A. Abdurahman, and T. Renger, J. Phys. Chem. B **110**, 17268 (2006).
[17] J. Neugebauer, J. Chem. Phys. **126**, 134116 (2007).
[18] B. Fückel, A. Köhn, M. E. Harding, G. Diezemann, G. Hinze, T. Basché, and J. Gauss, J. Chem. Phys. **128**, 074505 (2008).
[19] R. F. Fink, J. Pfister, H. M. Zhao, and B. Engels, Chem. Phys. **346**, 275 (2008).
[20] H.-C. Chen, Z.-Q. You, and C.-P. Hsu, J. Chem. Phys. **129**, 084708 (2008).
[21] M. E. Madjet, F. Müh, and T. Renger, J. Phys. Chem. B **113**, 12603 (2009).
[22] S. Yeganeh and T. Van Voorhis, J. Phys. Chem. C **114**, 20756 (2010).
[23] J. Vura-Weis, M. D. Newton, M. R. Wasielewski, and J. E. Subotnik, J. Phys. Chem. C **114**, 20449 (2010).
[24] T. Kawatsu, K. Matsuda, and J. Hasegawa, J. Phys. Chem. A **115**, 10814 (2011).
[25] A. A. Voityuk, J. Phys. Chem. C **117**, 2670 (2013).
[26] K. J. Fujimoto and S. Hayashi, J. Am. Chem. Soc. **131**, 14152 (2009).
[27] K. J. Fujimoto, J. Chem. Phys. **133**, 124101 (2010).
[28] K. J. Fujimoto, J. Chem. Phys. **137**, 034101 (2012).
[29] K. J. Fujimoto and C. Kitamura, J. Chem. Phys. **139**, 084511 (2013).
[30] K. Fujimoto and W.-T. Yang, J. Chem. Phys. **129**, 054102 (2008).
[31] B. H. Besler, K. M. Merz, Jr., and P. A. Kollman, J. Comput. Chem. **11**, 431 (1990).
[32] K. Hinsen and B. Roux, J. Comput. Chem. **18**, 368 (1997).
[33] H. C. Longuet-Higgins, Proc. R. Soc. London, Ser. A **235**, 537 (1956).
[34] R. McWeeny, *Methods of Molecular Quantum Mechanics*, 2nd ed. (Academic Press, London, 1989).
[35] R. D. Harcourt, G. D. Scholes, and K. P. Ghiggino, J. Chem. Phys. **101**, 10521 (1994).
[36] G. D. Scholes, R. D. Harcourt, and K. P. Ghiggino, J. Chem. Phys. **102**, 9574 (1995).
[37] A. D. Buckingham, Adv. Chem. Phys. **12**, 107 (1967).
[38] A. D. Buckingham, P. W. Fowler, and J. M. Huston, Chem. Rev. **88**, 963 (1988).
[39] P. W. Fowler and A. D. Buckingham, Chem. Phys. Lett. **176**, 11 (1991).
[40] P. Jurečka, J. Sponer, J. Černý, and P. Hobza, Phys. Chem. Chem. Phys. **8**, 1985 (2006).
[41] J. A. Pople, M. HeadGordon, and K. Raghavachari, J. Chem. Phys. **87**, 5968 (1987).
[42] R. A. Kendall, T. H. Dunning, Jr., and R. J. Harrison, J. Chem. Phys. **96**, 6796 (1992).
[43] T. H. Dunning, Jr., J. Chem. Phys. **90**, 1007 (1989).
[44] M. J. Frisch, G. W. Trucks, H. B. Schlegel *et al.*, Gaussian03, Revision B.04, Gaussian, Inc., Pittsburgh, PA, 2003.
[45] E. Runge and E. K. U. Gross, Phys. Rev. Lett. **52**, 997 (1984).
[46] M. E. Casida, in *Recent Advances in Density Functional Methods*, Part I, edited by D. P. Chong (World Scientific, Singapore, 1995), p. 155.
[47] J. B. Foresman, M. Head-Gordon, J. A. Pople, and M. J. Frisch, J. Chem. Phys. **96**, 135 (1992).
[48] A. J. Cohen, P. Mori-Sánchez, and W.-T. Yang, J. Chem. Phys. **126**, 191109 (2007).

This article is copyrighted as indicated in the article. Reuse of AIP content is subject to the terms at: http://scitation.aip.org/termsconditions. Downloaded to IP: 133.30.52.204 On: Thu, 04 Dec 2014 05:09:54